BBA - Molecular and Cell Biology of Lipids 1864 (2019) 158522

Contents lists available at ScienceDirect

BBA - Molecular and Cell Biology of Lipids

journal homepage: www.elsevier.com/locate/bbalip

Adaptation of *Synechococcus* sp. PCC 7942 to phosphate starvation by glycolipid accumulation and membrane lipid remodeling

Zhou Peng[a,b,c], Lei Feng[d], Xiaoxue Wang[e], Xiaoling Miao[a,b,c,*]

[a] State Key Laboratory of Microbial Metabolism and School of Life Sciences and Biotechnology, Shanghai Jiao Tong University, Shanghai 200240, China
[b] Joint International Research Laboratory of Metabolic and Developmental Sciences, Shanghai Jiao Tong University, Shanghai 200240, China
[c] Biomass Energy Research Center, Shanghai Jiao Tong University, Shanghai 200240, China
[d] Instrumental Analysis Center, Shanghai Jiao Tong University, Shanghai 200240, China
[e] School of Pharmacy, Shanghai Jiao Tong University, Shanghai 200240, China

ARTICLE INFO

Keywords:
Glycolipid
Phosphate stress
Lipidomic
Synechococcus sp. PCC 7942

ABSTRACT

Organisms use various adaptive strategies against phosphate stress, including lipid remodeling. Here, the response of major membrane lipids to phosphate stress was analyzed in *Synechococcus* sp. PCC 7942. Unlike plants and eukaryotic microalgae, no significant increases in neutral lipids were found, whereas glycolipids content increased to as high as 6.13% (of dry cell weight, DCW) and phospholipids decreased to 0.34% (of DCW) after 16 days of cultivation without phosphate. Glycolipids accumulation were mainly attributed to the significant increase of digalactosyldiacylglycerol (DGDG) by 50% and sulfoquinovosyldiaclglycerol (SQDG) by 90%, both of which acted as complementary lipids for phosphatidylglycerol (PG) in the cyanobacterial membrane. Also, a notable increase in content (by 48%) of C18 fatty acids (especially C18:1) was observed in all glycolipids at the expense of C12 and C14 (72%). These changes may contribute to membrane fluidity and photosynthetic activity for basic cell metabolism and phosphate stress adaptation. Lipidomic analyses showed the reduction of PG 18:1/16: 0 (by 52%) with the increase of DGDG 18:1/16:0 (133%) and SQDG 18:1/16:0 (245%), strongly suggesting a direct conversion of PG to DGDG and SQDG. Moreover, the decreasing amount of monogalactosyldiacylglycerol (MGDG) 16:1/16:0 (22%) was consistent with the increase of free fatty acids (125%) on day 2 of phosphate absence, which suggested that MGDG is more likely to provide a pool of fatty acids for de novo synthesis of glycolipids. This study provides valuable insight into cyanobacteria adaptation strategies to phosphate stress by membrane lipid remodeling and unveils the underlying acyl chain fluxes into glycolipids.

1. Introduction

Glycolipids are widely found in plants, microalgae, and cyanobacteria, and a few members of Gram-positive and Gram-negative bacteria [1]. They not only serve as structural lipids, which determine the fluidity and integrity of membranes, but are also sensitive to changes in the environment [2,3], such as temperature changes [4] and nutrient deficiency [5]. Phosphorus is a necessary element for organisms to maintain normal growth. Reduced phosphate concentration affects cell growth, pigment content, photosynthetic activity, nucleotide and phospholipids synthesis, DNA assembly, and other physiological changes in the cell [6]. Organisms have developed different mechanisms to deal with phosphate stress conditions. Phosphate deprivation conditions result in induced expression for several genes, leading to an increasing level of phosphorous transport and uptake capacity [7,8]. The elevation of RNase gene expression level stimulates RNA degradation, which releases phosphorus for other physiological processes in the cell [9]. The remodeling of lipids is another vital process for cell

Abbreviations: Chl, chlorophyll; DAG, diacylglycerol; DGDG, digalactosyldiacylglycerol; ESI, electrospray ionization; FFAs, free fatty acids; FAMEs, fatty acid methyl esters; G3P, Glyceraldehyde 3-phosphate; GGD, glucosylgalactosyldiacylglycerol; GlcADG, glucuronosyldiacylglycerol; MAG, monoacylglycerol; MGDG, monogalactosyldiacylglycerol; PE, Phycoerythrin; PC, Phycocyanin; PG, phosphatidylglycerol; SQDG, sulfoquinovosyldiaclglycerol; TAG, triacylglycerol; TEM, transmission electron microscopy; TLC-GC, thin layer chromatography-gas chromatography; UPLC-MS, ultra-performance liquid chromatography-mass spectrometry; UHPLC-MS, ultra-high performance liquid chromatography-mass spectrometry

* Corresponding author at: State Key Laboratory of Microbial Metabolism and School of Life Sciences and Biotechnology, Shanghai Jiao Tong University, Shanghai 200240, China.

E-mail addresses: pengzhou@sjtu.edu.cn (Z. Peng), fiona.fenglei@sjtu.edu.cn (L. Feng), wangxiaoxue@sjtu.edu.cn (X. Wang), miaoxiaoling@sjtu.edu.cn (X. Miao).

https://doi.org/10.1016/j.bbalip.2019.158522
Received 20 June 2019; Received in revised form 22 August 2019; Accepted 29 August 2019
Available online 02 September 2019
1388-1981/

growth during phosphate deprivation.

In plants and microalgae, glycolipids monogalactosyldiacylglycerol (MGDG), digalactosyldiacylglycerol (DGDG) and sulfoquinovosyldiaclglycerol (SQDG) are the main components of the plastid membrane and are essential in chloroplast functions, whereas phospholipids are the main subcellular membrane lipid class under replete nutrient conditions [1]. In phosphate-starved conditions, the amounts of DGDG and SQDG increase at the expense of phospholipids in plants [1,10–12]. UPLC-MS(/MS)- and UPLC-MS/MS(/MS)-based lipidomic analyses further reveal that phospholipids are broken down to glyceraldehyde-3-phosphate (G3P), fatty acids, and diacylglycerol (DAG) [13]. The products are used to synthesize triacylglycerol (TAG), diacylglycerol-*N*,*N*,*N*-trimethylhomoserine (DGTS), and glycolipids (MGDG, DGDG, and SQDG) [13]. These changes suggest an effective phosphorus-conserving mechanism for cell survival. Moreover, the accumulation of a new class of glycolipid glucuronosyldiacylglycerol (GlcADG) in plants has also been suggested as essential in protecting against phosphorus depletion [14–16]. In addition, Gram-negative bacteria (*Sinorhizobium meliloti* and *Rhodobacter sphaeroides*) accumulate ornithine lipids (OL) and DGTS during phosphate limitation [17–19]. Other cases involved in DGTS accumulation are found in some microalgae, such as *Chlamydomonas reinhardtii* [20] and *Nannochloropsis* [21]. In addition, *Rhodobacter* also accumulates glucosylgalactosyldiacylglycerol (GGD), which is a unique glycolipid with α-glucose (1 → 4) linked to β-galactose [22]. These findings demonstrate that organisms can synthesize substitute lipids in response to phosphorus limitation, which is essential for them to adapt to phosphorus scarcity.

Cyanobacteria are widely spread across the world and make up to 25% of primary production in the oceans [23]. Their biomass concentration is usually limited by supplementation and recycling of nutrients, especially phosphorus [24]. Cyanobacteria spread from the poles to the equator [25], suggesting that these organisms have developed efficient mechanisms to adapt to phosphate variations. A systematic investigation of glycolipids in the Adriatic Sea revealed that increased glycolipids instead of phospholipids are common in oligotrophic ocean areas, particularly in phosphate limited regions, representing an effective phosphorus conserving strategy for plankton survival, including cyanobacteria [26]. So far, although it has been suggested that SQDG and DGDG can be induced under phosphate-depleted conditions in cyanobacteria [27–30], a detailed adaptation mechanism for lipid remodeling has not been unveiled. To understand how cyanobacteria adapt to phosphate stress by lipid remodeling, we investigated lipid class, membrane lipid composition, and fatty acid profile changes of *Synechococcus* sp. PCC 7942 under phosphate-starved conditions. Moreover, an analysis using an ultra-high performance liquid chromatography mass spectrometry (UHPLC-MS)-based lipidomic platform further helped us understand the DAG and acyl flux underlying this lipid remodeling mechanism.

2. Materials and methods

2.1. Algae culture and experimental design

Synechococcus sp. PCC 7942 was obtained from Shanghai Ocean University of China. Cells were air bubbled under 25 ± 2 °C and 140 μmol $m^{-2} s^{-1}$ in a 1 L Erlenmeyer flask (20 cm length, 10 cm diameter) with 500 mL working volume of modified BG11 medium. The initial OD_{730} was 0.1 and the pH was 8.0 [31].

In the experiments to study the effect of different phosphate concentrations on cell growth, photosynthesis activities, and lipid content, 1 L cell culture obtained at the end of the linear growth phase was harvested by centrifugation (8000 rpm, 15 min) and washed twice with sterilized water. Cells were diluted by adding 100 mL non-phosphate BG11 medium and transferred into fresh BG11 medium with different initial phosphate concentrations (0.08, 0.04, 0.03, 0.02, 0.01, and 0 g L^{-1}). The initial OD_{730} was 0.1. Cell growth and photosynthesis activities were measured every two days from day 0 to day 18. Cells grown under different phosphate concentrations were harvested on day 18, then washed with methanol (10%, v/v) and stored at −80 °C for the subsequent lipid analyses.

To study the effect of phosphate starvation (0 g L^{-1}) on dynamic changes of lipids, cells were grown in BG11 medium with a phosphate concentration of 0.04 g L^{-1} (+P) or 0 g L^{-1} (−P). The culture conditions and procedures were carried out as described above. Cells were harvested every two days from day 0 to day 16.

2.2. Growth and biomass concentration determination

According to the method of Chiu et al. [32] the dry cell weight (DCW) was determined. *Synechococcus* sp. PCC 7942 were harvested by centrifugation, and washed twice. To determine DCW, the cell pellet was lyophilized using a freeze drier (FD-1-50, Boyikang, China). A calibration curve of OD_{730} measured by spectrophotometer (UV-1000, Techcom, China) versus cell density was constructed. The sample was diluted to an OD_{730} ranging from 0.1 to 1.0. Biomass concentration of *Synechococcus* sp. PCC 7942 was calculated using the following equation: Biomass concentration (g L^{-1}) = 0.274 × OD_{730} + 0.0202 (R^2 = 0.990). Therefore, the biomass concentration was precisely predicted by optical density. The DCWs were means of three independent experiments.

2.3. Photosynthetic activity analysis

Chlorophyll was determined after its extraction from the cells with 90% (v/v) methanol [33]. One-half milliliter of cell suspension was centrifuged (10,000 *g*) at 4 °C for 10 min, then the chlorophyll of the pellet was extracted twice with methanol (90%, v/v) at 4 °C in dim light for 1 h. After centrifugation (10,000 *g*) at 4 °C for 10 min, the content of chlorophyll was calculated according to the absorbance value of the methanol extracts by using a spectrophotometer (UV-1000, Techcom, China), with Eq. (1).

$$C\ (\mu g\ mL^{-1}) = OD_{665} \times 13.9 \quad (1)$$

The fluorescence emission spectra were studied with a spectrofluorometer (LS-55, Perkin-Elmer, Germany). The phycoerythrin to phycocyanin ratio (PE:PC) was determined by recording the fluorescence excitation spectra [34].

The photosystem II quantum yield (F_V/F_M) was recorded by a Pulse Amplitude Modulation fluorometer (PhytoPAM, Walz, Effeltrich, Germany) before a dark period of 300 s, following a previously described procedure [34]. The value was calculated as: $F_V/F_M = (F_V\text{-}F_0)/F_M$, where F_0 is the basal fluorescence level, F_M is the maximal fluorescence level and F_V is the variable fluorescence.

2.4. Total lipid extraction and fractionation

Total lipids were extracted according to the modified method of Zhu et al. [35]. Ground, dry cyanobacteria power (200 mg) was suspended in chloroform:methanol (2:1, v/v) at the volume of 10 mL. Samples were centrifuged (10 min, 8000 rpm) after extraction for 10 min. This step was repeated another two times until the lipids were fully extracted. The supernatant organic solvent was moved to an empty tube and evaporated to dryness in water at 65 °C. The contents of total lipids were measured (BS 124S, Sartorius, Germany).

The extracted total lipids were separated into neutral, glyco-, and phospho-lipids using silica Sep-Pak cartridges (500 mg, Waters, USA) as described by Damiani et al. [36]. First, the silica cartridges were equilibrated with methanol (100%, 10 mL), followed by chloroform (30 mL). Subsequently, 20 mg total lipids (contained in 1 mL chloroform solution) were added to the cartridges. The neutral lipids fraction was first collected by eluting with chloroform:acetic acid (9:1, v/v) at the volume of 15 mL. The glycolipids fraction was collected by eluting

with acetone:methanol (9:1, v/v) at the volume of 20 mL. The phospholipids fraction was collected last by eluting with 20 mL methanol. The amounts of neutral, glyco- and phospho-lipids were measured by weighing after drying in a rotary evaporator (N-1100V-W, EYELA, Japan) at 60 °C under vacuum.

2.5. Lipid composition and fatty acids profile analysis

Total lipids of the cells cultivated in −P/+P cultures on day 16 were chosen for further lipid composition and fatty acid analysis by thin layer chromatography (TLC) coupled with gas chromatography mass spectrometry (GC–MS). Detailed processes were as follows. A silica TLC plate (Merck, Germany) was dipped in 0.15 M ammonium sulfate solution for 30 s and then dried for more than two days. A solution of acetone:toluene:water (91:30:7, v/v/v) was the developing solvent [12]. After developing, the total lipids were separated into four main classes (MGDG, DGDG, SQDG, and PG). Spots were visualized by iodine or α-naphthol staining. The position of each lipid class on the TLC plate was confirmed by comparing with lipid standards (Avanti Polar Lipids, USA).

For lipid composition and fatty acid analysis, each spot was scraped from the plate and transferred into a glass tube. To the samples, 5 μg nonadecanoic acid (C19:0) in 0.1 mL methanol was added as an internal standard. Fatty acid methyl esters (FAMEs) were prepared by adding 1 mL 1 N methanolic HCl followed by incubation at 80 °C for 1 h. Following the addition of 1 mL 0.98% (wt/vol) KCl, the FAMEs were extracted by hexane (1 mL) and then concentrated to a small volume (0.1 mL). Samples were injected into an AutoSystem XL GC/TurboMass MS (Perkin Elmer, Germany) for further GC–MS analysis [37]. A Spectra Physics integrator was used for the integration of fatty acid data. The contents of fatty acids of each lipid class were calculated based on the assumption that each lipid class contained two fatty acids per molecule. For example, to calculate the DGDG content, we used Eq. (2) [12]. Three independent experiments were conducted.

$$(\mathrm{DGDG})\ \mathrm{mol\%} = \sum [\mathrm{FAMEs}_{(\mathrm{DGDG})}] / \sum [\mathrm{FAMEs}_{(\mathrm{total})}] \times 100\% \quad (2)$$

2.6. Reversed phase chromatography

A Vanquish UHPLC system equipped with an ACQUITY UPLC BEH C18 column (100 × 2.1 mm, 1.7 μm, Waters) was used to separate lipid substances based on a modified method of Su et al. [38]. Mobile phases were acetonitrile:water (60/40, v/v) with 10 mM ammonium formate and 0.1% formic acid (A) and isopropanol:acetonitrile (90/10, v/v) with 10 mM ammonium formate and 0.1% formic acid (B). The following gradient was used at a flow rate of 0.4 mL min^{-1}: 0–0.5 min 95% A, 2–2.1 min 57% A, 12 min 50% A, 12.1 min 46% A, 18 min 30% A, and 18.1–20 min 95% A. The injection volume was set to 1 μL and the column temperature was set to 55 °C.

2.7. Q Exactive plus mass spectrometer for identification of lipids

As described by Criscuolo et al. [39], a Thermo Scientific Q Exactive hybrid quadrupole-Orbitrap mass spectrometer with electrospray ionization source (ESI) was used in data dependent mode (DDA) with one full mass scan followed by the top 10 MS/MS scans per cycle. Spray voltage was set to 3.2 kV in positive ion mode and 2.8 kV in the negative ion mode, all other interface settings were identical for positive and negative ion modes. The capillary temperature, aux gas heater temperature, sheath gas flow, aux gas flow, and s-lens RF level were set at 320 °C, 350 °C, 50 Arb, 15 Arb, and 50 V, respectively. For full mass acquisition, data were collected in the range of m/z 150–2000 with 70,000 resolution. The value of automatic gain control (AGC) and the maximum injection time (IT) were 1e6 and 100 ms, respectively. For data dependent MS/MS acquisition, spectral information was acquired with a resolution of 17,500, AGC of 5e5, and IT of 50 ms. Over the whole collecting process, nitrogen (99.999%) was used as a collision-induced dissociation gas. The normalized collision energy (NCE) was 15, 30, and 45 to fragment ions. Additives, high resolution mass, and fragmentation of membrane lipids were used for identification according to the fragmentation pattern of the standards (MGDG, DGDG, SQDG, and PG 17:0/14:1 (Avanti Polar Lipids, USA)). In this experiment, MGDG, DGDG, SQDG and PG were more suitable in negative mode than positive, hence negative mode was used for identifying those lipids (Fig. S1, Tables S1 and S2). However, DAG and TAG were more suitable for positive mode than negative. Identification (Table S3) was according to the method described by Légeret et al. [4].

Quantification of lipid molecular species was according to a modified method described by Yang et al. [40]. The lipid molecular species were further quantified through external standard calibration. The equations between lipid standard concentrations and peak areas were shown in Table S4. The lipid standards were MGDG, DGDG, SQDG, PG 17:0/14:1, DAG 18:1/18:1, and TAG 18:1/18:1/18:1 from Avanti Polar Lipids (USA). Three independent biological replicates were analyzed.

2.8. Data processing

The UHPLC-MS(/MS) data were obtained in raw files with the XCalibur software (Thermo Fisher Scientific). The identification, alignment and quantification were conducted using LipidSearch™ 4.1 (Thermo Fisher). The identification of lipids was determined by the comparison of the fragmentation ions, the retention time and high resolution mass, which reveal the fatty acyl groups (FAs) on lipids, using the LipidSearch Database. The sample names (based on the retention time, peak feature, and m/z) and normalized peak intensity were exported for principal components analysis (PCA) using SIMCA software (V.12.0, Umetric, Sweden). Three independent biological replicates were analyzed.

2.9. Ultrastructure observation

The ultrastructure of cells was determined using transmission electron microscopy (TEM). Sample were fixed in 2.5% glutaraldehyde in 0.1 M phosphate buffer (pH 7.4) at 4 °C for at least 7 h and then postfixed in 2% osmium tetroxide in the same buffer. Cells were dehydrated through an ethanol series, and then embedded in epoxy resin. Ultra-thin sections were cut using an ultramicrotome (Leica EM UC7, USA) with a diamond knife and stained with uranyl acetate followed by lead citrate solution. The images were taken with a transmission electron microscope (Tecnai G2 spirit Biotwin, CZ).

2.10. Membrane fluidity measurement

The membrane fluidity was estimated by measuring the steady-state fluorescence polarization of the hydrophobic probe 1,6-diphenyl-1,3,5-hexatriene (DPH). Thylakoid membranes were separated from *Synechococcus* sp. PCC 7942 cells according to the method described by Kondo et al. [41]. Cells were harvested and then suspended in 1 mM HEPES (pH 7.5) containing 0.1 M sorbitol and 10 mM KCl [42]. Cells were broken using a Beadbeater (Tissuelyser-24, Jingxin, China) with zirconia/silica beads (0.1 mm, Biospec, USA). Then, thylakoid membranes were precipitated by centrifugation at 20,000 × g for 30 min. Next, the membranes were suspended in PBS (pH 7.4) (1 mL of 1 μg chlorophyll) and labeled with DPH (0.2 μM) [43] on ice in the dark for 1 h. Thylakoid membranes labeled with DPH were incubated at 20 °C in the dark for 10 min, and then, the fluorescence polarization of the labeled membranes were measured using a fluorescence spectrophotometer (FLS1000, Edinburgh, UK) between 20 °C and 50 °C, with an excitation light of 380 nm (4 nm slit) and emission light of 425 nm (7 nm slit). The polarization values were calculated as described by Barber et al. [42].

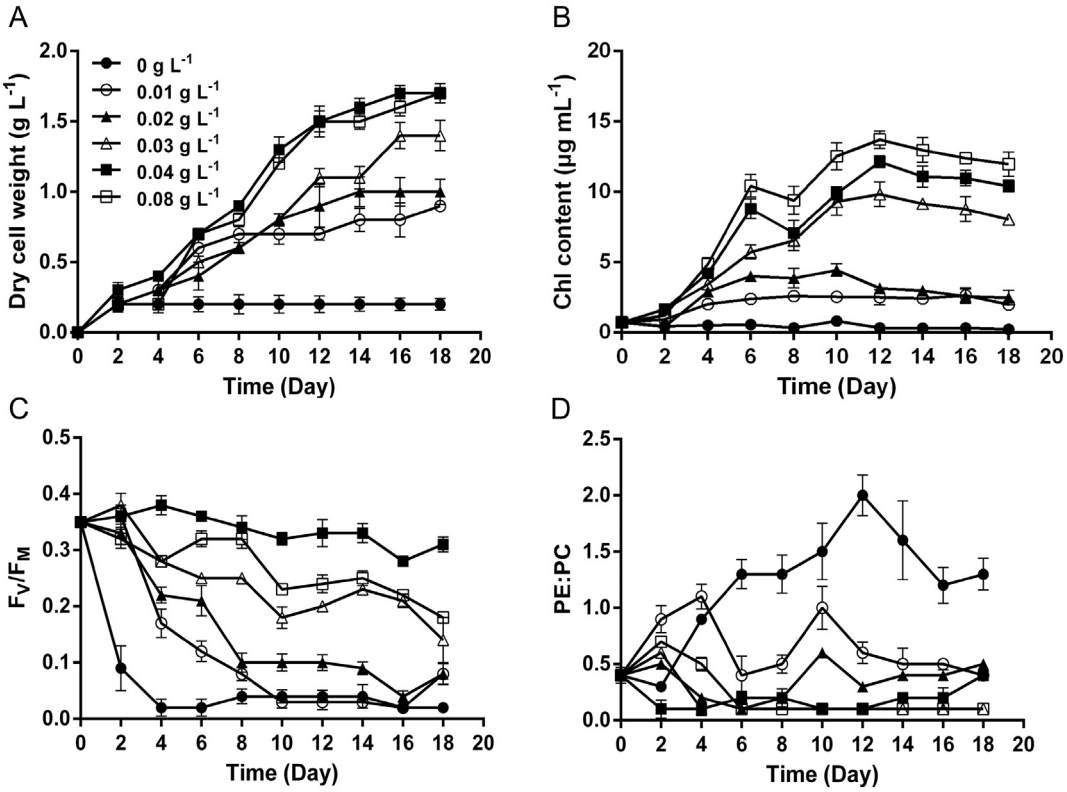

Fig. 1. The growth and photosynthesis activities of *Synechococcus* sp. PCC 7942 in modified BG11 medium at different phosphate concentrations. Dry cell weight (DCW) (A), chlorophyll (Chl) content (B), photosystem II quantum yield (F_V/F_M) (C), and phycobiliprotein fluorescence emission ratio (PE:PC) (D). Mean, n = 3. PE, phycoerythrin; PC, phycocyanin.

3. Results

3.1. Growth and photosynthesis activities of Synechococcus sp. PCC 7942 under different phosphate concentrations

The growth and photosynthesis activities of *Synechococcus* sp. PCC 7942 under different phosphate concentrations are shown in Fig. 1. The growth of cyanobacteria was retarded under phosphate stressed or starved conditions (Fig. 1A). Under phosphate depleted conditions (0 g L^{-1}), the biomass concentration increased to the highest content (0.2 g L^{-1}) on day 2 and remained constant until day 18 (Fig. 1A). When cells were grown under phosphate stress conditions (0.01, 0.02, 0.03 g L^{-1}), the biomass concentration showed a slower increase than those grown under phosphate replete conditions (0.04, 0.08 g L^{-1}) (Fig. 1A). This indicated that cells can still grow under phosphate stressed or starved conditions. In parallel, similar patterns were detected for the chlorophyll content (Fig. 1B). The synthesis of chlorophyll was almost completely inhibited in cells grown without phosphate (Fig. 1B). However, the chlorophyll contents showed a relatively slower increase under phosphate stress (0.01, 0.02, 0.03 g L^{-1}) conditions than those under phosphate replete conditions (0.04, 0.08 g L^{-1}) (Fig. 1B). The chlorophyll content of the cells reached 9.3 (μg mL^{-1}) under 0.03 g L^{-1} phosphate concentration on day 10, which was almost the same as those grown under 0.04 g L^{-1} phosphate concentration at the same time (Fig. 1B). Moreover, the photosynthetic quantum yield (F_V/F_M) value was almost constant (0.35) during the entire experiment under 0.04 g L^{-1} phosphate concentration, whereas it was significantly decreased throughout the experiment under phosphate stressed or starved conditions (Fig. 1C), which indicated a drop in photosynthetic capacity under phosphate stress conditions. The results above suggested that although chlorophyll synthesis and photosynthesis activities were repressed under phosphate stress conditions, the cells kept growing with relatively low photosynthetic activities.

The phycobiliprotein fluorescence excitation ratio (phycoerythrin:phycocyanin, PE:PC) reflects the adjustment of light utilization capacity [44]. Cells grown under phosphate absent conditions had a higher PE:PC value than those grown under phosphate replete conditions (0.04, 0.08 g L^{-1}) (Fig. 1D). The PE:PC value of cells grown with no phosphate increased significantly from 0.4 (day 0) to 1.9 (day 12) and then gradually decreased to 1.2 (day 18) (Fig. 1D). This sharp turnover pattern was also found on day 10 in cells grown under phosphate stress (0.01 and 0.02 g L^{-1}) conditions (Fig. 1D). This demonstrated the up-regulation of light utilization capacity in cyanobacterial cells grown under phosphate stress conditions. The results above indicated that *Synechococcus* sp. PCC 7942 could be kept alive under phosphate stress, and even without phosphate, and have the ability to adjust photosynthetic activities and light utilization to adapt to phosphate stress.

3.2. Changes of lipid class in response to different phosphate concentrations in Synechococcus sp. PCC 7942

To explore the relationship between lipid changes and phosphate-stress adaptation, the contents of total lipids and different lipid classes in *Synechococcus* sp. PCC 7942 under different phosphate concentrations were determined. As shown in Fig. 2, the contents of total lipids and neutral lipids did not have significant changes, while contents of glycolipids and phospholipids changed significantly. The content of glycolipids increased with reduced phosphate concentrations, reaching 5.58% in cells grown without phosphate, which was 1.7-fold higher than that of the control (0.04 g L^{-1}) (Fig. 2). However, the content of phospholipids decreased with the reduction of phosphate concentrations. The lowest content (0.42%) of the phospholipids was observed under phosphate absence, which was > 74% decreased as compared with that of the control (Fig. 2). The results suggested that phosphate limitation, especially starvation, may induce the alteration of lipid

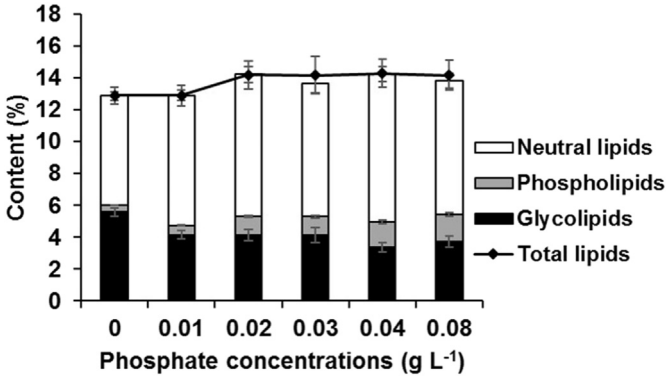

Fig. 2. Effects of different phosphate concentrations in contents (% DCW) of total lipids, neutral lipids, glycolipids and phospholipids in of *Synechococcus* sp. PCC 7942. Cells were cultivated in modified BG11 medium for 18 days. Mean, n = 3.

composition in cyanobacteria.

To further understand the lipid changes during the whole growth period, time-course changes of each lipid class under 0 g L^{-1} (−P) and 0.04 g L^{-1} (+P) phosphate concentrations were analyzed (Fig. 3). The total lipids and neutral lipids in −P cultures did not show any significant changes over the whole growth period (Fig. 3A and B). However, glycolipids had an increasing trend over all growth stages, especially from day 12 to day 16, and reached the highest content of 6.13% in −P cultures on day 16, which was 1.95-fold higher than that in +P cultures (Fig. 3C). Phospholipids reached its maximal content of 3.01% on day 2, and decreased to 1.22% on day 8, and then slowly declined to 0.34% on day 18 (Fig. 3D). Glycolipids and phospholipids are the main structural components of thylakoid and cytoplasmic membranes [45]. The results indicated that phosphate starvation may induce significant membrane lipid changes, especially on day 16.

3.3. Effect of phosphate limitation on membrane lipid composition

Glycolipids (MGDG, DGDG, and SQDG) and phosphatidylglycerol (PG) exist in oxygenic photosynthetic organisms from cyanobacteria to higher plants, and contribute to constructing membrane systems, including thylakoid membranes [46–48]. To further understand the effect of phosphate stress on membrane lipid composition, we chose cells grown on day 16 for membrane lipids analysis, when the glycolipid content was the highest (Fig. 3C). Membrane lipid composition varied significantly. As shown in Fig. 4B, the DGDG and SQDG contents in −P cells increased respectively 1.5-fold and 1.9-fold compared with that in +P cells. The proportion of membrane phospholipid (PG) was decreased by 75% in −P cells compared with that in +P cells (Fig. 4B). This suggested that DGDG and SQDG may act as substitute lipids for PG under −P conditions and that lipid remodeling occurred. This remodeling, where phospholipids were replaced with non-phospholipids, has also been found in bacteria, plants and several microalgae [49–51].

The supply of phosphate also affects the fatty acid composition of membrane lipids. In −P cells, C18:1 fatty acid showed clear increases in MGDG, DGDG and SQDG, which increased by 149%, 106% and 421%, respectively, compared with that in +P cultures (Table 1). The total content of medium-chain fatty acids (C14:1, C14:0 and C12:0) was decreased by 72% compared with that of the control (calculated from Table 1). This suggested that fatty acid synthesis and elongation happened under phosphate-starved conditions. There was almost no

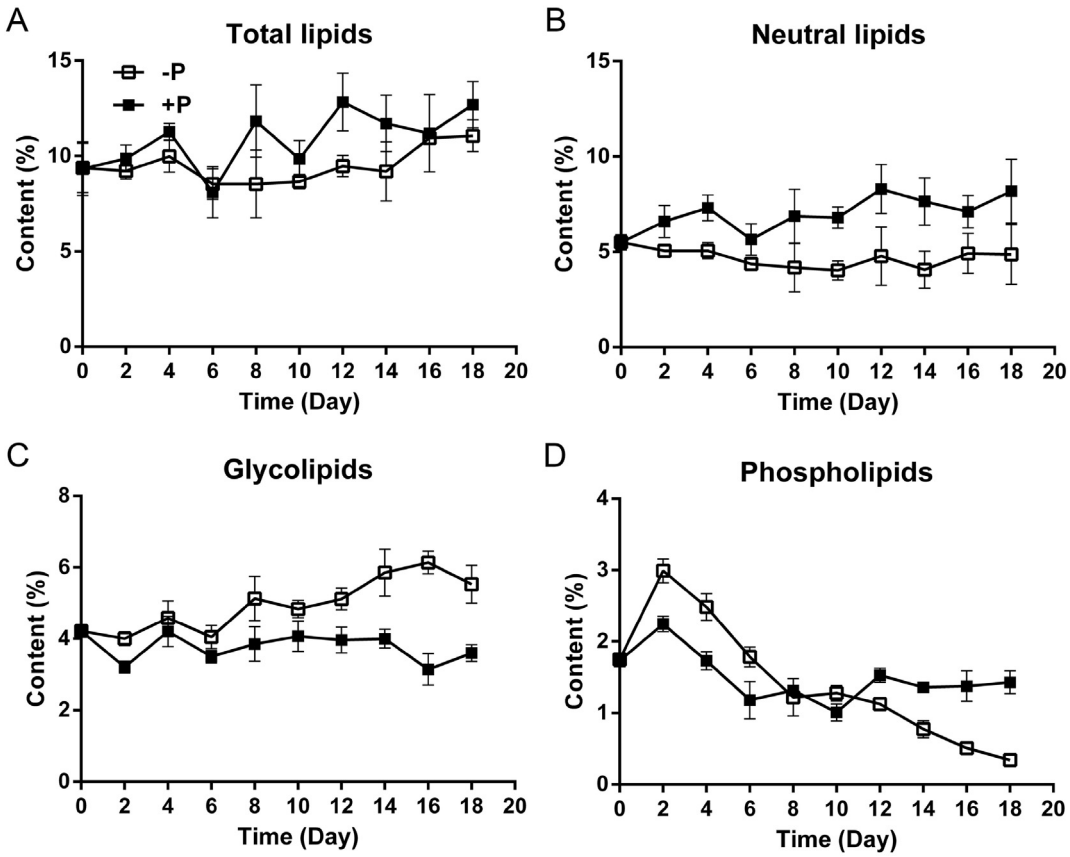

Fig. 3. Dynamic changes in contents (% DCW) of total lipids (A), neutral lipids (B), glycolipids (C), and phospholipids (D) in *Synechococcus* sp. PCC 7942 under phosphate replete (+P) and phosphate depleted (−P) conditions. Mean, n = 3. The legends, +P and −P, indicate phosphate concentrations in the medium of 0.04 g L^{-1} and 0 g L^{-1}, respectively.

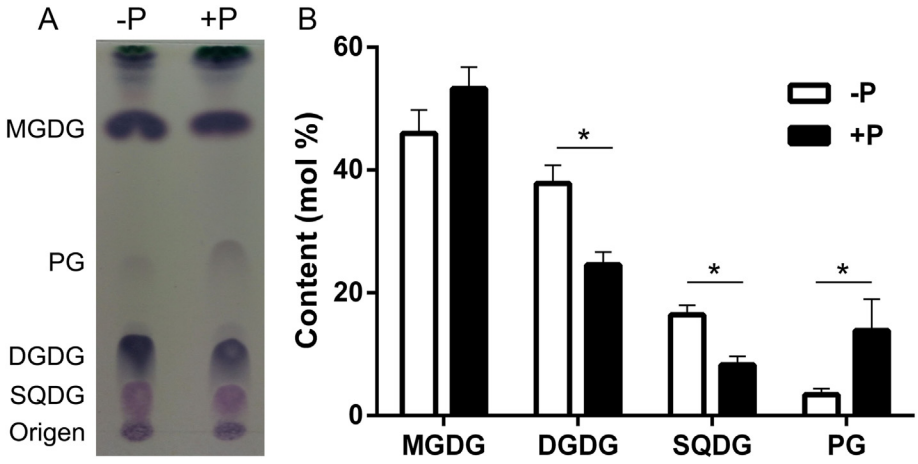

Fig. 4. Membrane lipid composition of *Synechococcus* sp. PCC 7942 grown under phosphate depleted (−P) and replete (+P) conditions for 16 days. Total lipids separation by TLC and visualization by α-naphthol staining (A); Content of each membrane lipid class (B). Mean, n = 3. Student's *t*-test (*P < 0.05). The legends, +P and −P, indicate phosphate concentrations in the medium of 0.04 g L^{-1} and 0 g L^{-1}, respectively.

difference in the fatty acid composition of PG between −P and +P cells (Table 1). One possible reason was that PG mainly donates DAG for glycolipids synthesis. The results above suggested that the phosphate stress-induced membrane lipid remodeling and changes in fatty acid composition seemed to alter the membrane fluidity and stability and help cyanobacteria adapt to unfavorable conditions.

3.4. Effect of phosphate limitation on membrane thickness and fluidity

The internal ultrastructures of *Synechococcus* sp. PCC 7942 cells under phosphate replete (+P) and depleted (−P) conditions were further observed using transmission electron microscopy (TEM) (Fig. 5). As shown in Fig. 5B, the thylakoid membrane was considerably thicker in −P cells than that in +P cells (Fig. 5A) after 16 days of phosphate starvation. The thicker membrane resulted in a stacked formation in −P cells. The superficial area of the thylakoid membrane seemed expanded in −P cells (Fig. 5B). These alterations were similar to those seen in *Scenedesmus* [52] and *Phaeodactylum tricornutum* [53] under phosphate stress conditions. Many small polyphosphate bodies (PPBs) adhering to DNA were observed in +P cells (Fig. 5A); however, the PPBs were almost absent in −P cells (Fig. 5B). This indicated that the degradation of PPBs might be involved in providing phosphorus for DNA replication under −P condition [54,55].

Changes in fatty acid composition of membrane lipids directly affect thylakoid membrane fluidity [56]. The fluorescence polarization of DPH in membranes separated from −P and +P cells were therefore measured (Fig. 6). The polarization of DPH fluorescence in −P cells was lower than that in +P cells (Fig. 6), which suggested an increased membrane fluidity in *Synechococcus* sp. PCC 7942 over 16 days of phosphate starvation.

3.5. Lipidomic analysis of Synechococcus sp. PCC 7942

To decipher how membrane lipids were remodeled under phosphate stress conditions, an UHPLC-MS(/MS)-based lipidomic approach was adopted. We could distinguish five major lipid classes and free fatty acid (FFA) profiles with different molecular species in the cells. Our analysis identified fifteen MGDG, fifteen DGDG, and ten SQDG molecular species. The PG lipid class contained 21 molecular species (Table S2). DAG exhibited nine identified molecular species (Table S3). FFA was present in five different molecular species. Among those lipid classes, we also distinguished regiochemical distribution of the sn-1/sn-2 acyl chains of MGDG, DGDG, SQDG, and PG (Table S2).

To reveal the clustering trends within our multivariate lipidomic data, an unsupervised statistical method (principal component analysis, PCA) was used. In a PCA, differences and similarities of the samples are revealed in the score plots by analysis of pattern formations or two-dimensional clustering [38]. The first two components, which are used for plotting scores and loadings, explained 77.0% of the variance (Fig. 7). In the score plot (Fig. 7), the cells grown under −P conditions were separated clearly during different growth days. However, cells grown under +P conditions were clustered in one area of the plot from day 2 to day 16 (Fig. 7), which indicated no significant physiological differences in +P cultures. The result indicated that different metabolites occurred under −P conditions. Therefore, based on the PCA analysis above, we chose lipidomic data of −P cells from day 0 to day 16 for the next analysis.

To reveal the more specific role of PG in glycolipid accumulation, such as providing acyl groups and diacylglycerol (DAG) for glycolipid assembly, the changes of their molecular species during 16 days of phosphate starvation were further investigated (Fig. 8). Multiple

Table 1
Fatty acid composition of each individual membrane lipid class in *Synechococcus* sp. PCC 7942 grown in phosphate-starved condition for 16 days. Cells were cultivated in modified BG11 medium under phosphate replete (+P) and phosphate depleted (−P) conditions. Mean, n = 3. Student's *t*-test (*P < 0.05). The legends, +P and −P, indicate phosphate concentrations in the medium of 0.04 g L^{-1} and 0 g L^{-1}, respectively.

Fatty acid (mol %)	MGDG		DGDG		SQDG		PG	
	−P	+P	−P	+P	−P	+P	−P	+P
12:0	2.84 ± 0.08*	9.21 ± 1.21	n.d. *	0.11 ± 0.03	n.d.	n.d.	n.d.	n.d.
14:0	n.d. *	0.15 ± 0.02	n.d. *	1.62 ± 0.27	0.03 ± 0.01*	2.15 ± 0.19	n.d.	n.d.
14:1	0.51 ± 0.31*	4.01 ± 1.02	0.19 ± 0.04*	2.50 ± 0.18	n.d. *	0.08 ± 0.03	0.90 ± 0.13	1.01 ± 0.06
16:0	43.71 ± 4.47	56.22 ± 8.17	40.74 ± 4.88	45.97 ± 3.56	43.39 ± 4.11	42.48 ± 3.08	45.35 ± 1.58	47.34 ± 3.28
16:1	22.75 ± 6.02	19.14 ± 4.49	35.79 ± 2.53	39.49 ± 1.83	42.92 ± 2.85	36.74 ± 2.79	9.66 ± 0.20	8.54 ± 0.94
17:1	n.d.	n.d.	n.d.	n.d.	n.d.	n.d.	0.55 ± 0.12	0.25 ± 0.08
18:0	0.90 ± 0.12*	n.d.	2.41 ± 0.59*	0.53 ± 0.12	n.d. *	14.91 ± 1.79	1.71 ± 0.39	2.26 ± 0.42
18:1	29.70 ± 2.27*	11.91 ± 2.00	19.39 ± 1.30*	9.40 ± 2.51	11.94 ± 1.82*	2.29 ± 0.68	37.41 ± 3.42	39.03 ± 1.32
18:2	n.d.	n.d.	n.d.	n.d.	n.d.	n.d.	4.10 ± 0.42*	2.30 ± 0.32

n.d., not detected.

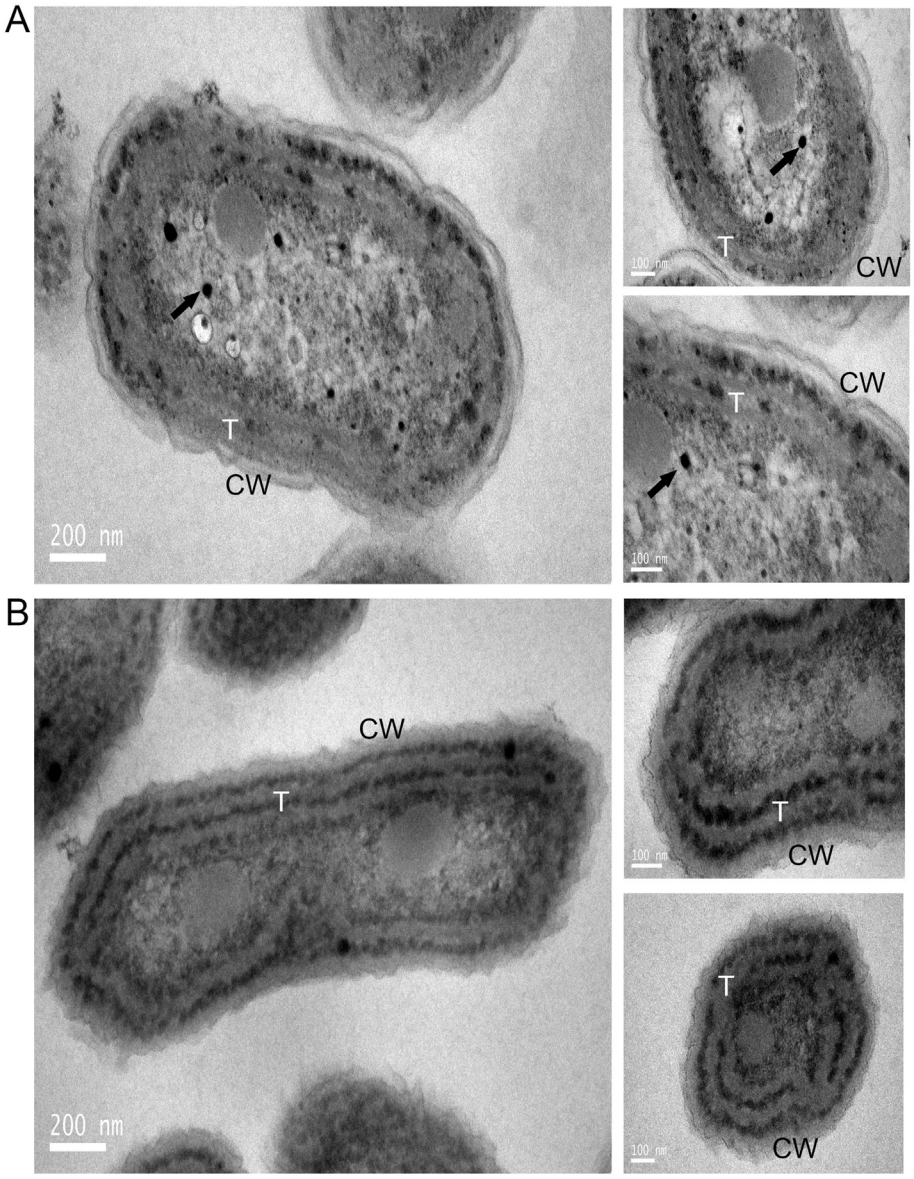

Fig. 5. TEM images of *Synechococcus* sp. PCC 7942 cells grown in phosphate replete (+P) (A) and phosphate depleted (−P) (B) conditions for 16 days. The black arrowhead in A indicates polyphosphate bodies (PPBs). T, thylakoid membrane; CW, cell wall. The legends, +P and −P, indicate phosphate concentrations in the medium of 0.04 g L^{-1} and 0 g L^{-1}, respectively.

changes of these five glycerolipid molecular species are presented in Fig. 8. MGDG molecular species were selectively degraded, i.e., 16:1/16:0, 12:0/16:0, 14:1/16:0, and 16:0/16:0, among which the main proportion 16:1/16:0 decreased the most (by 22%) during 2 days of phosphate stress and then remained unchanged (Fig. 8A). Some molecular species of MGDG gradually increased during 16 days of phosphate deprivation, i.e., 18:1/16:1, 18:1/16:0, and 18:1/18:1, of which 18:1/16:0 contributed > 80% to increased MGDG (Fig. 8A). The result indicated that the acyl chain varied in MGDG during phosphate stress conditions. The major PG molecular species included 16:1/16:0 and 18:1/16:0, both of which decreased by 75% and 52%, respectively, after 16 days of phosphate starvation (Fig. 8D). This change was consistent with the elevation of DAG molecules on day 8, i.e. 16:1/16:0, 18:1/16:0 and 18:1/16:1, which increased by 59%, 289% and 157%, respectively (Fig. 8E). This suggested that the conversion of PG to DAG took place during the eight phosphate-starvation days. Moreover, the total FFA content increased significantly by 125% on day 2 and then sharply decreased by 63% on day 16 (Fig. 8F). It seemed that DAG and FFA functioned as mediators for glycolipid assembly, in particular DGDG 18:1/16:0 and SQDG 18:1/16:0, which increased 133% and 245%, respectively (Fig. 8B and C). This results above demonstrated a membrane lipid remodeling scenario where the initial degradation of PG and MGDG mainly provide DAG or fatty acid pools for glycolipid accumulation and membrane lipid remodeling.

4. Discussion

4.1. Growth and photosynthesis changes reflect phosphate stress adaptation

It has been widely accepted that environmental stress (such as phosphate [13,51], nitrate [45,51], sulfite [57], and temperature stress [34]) reduce pigment content, photosynthetic activities, and cell growth. In our study, photosynthetic activities and growth of *Synechococcus* sp. PCC 7942 were also inhibited because of phosphate depletion (Fig. 1A). The downregulation of growth rate and pigment content has been suggested as a protective mechanism for cells [58]. In our study, *Synechococcus* sp. PCC 7942 kept growing under phosphate stress, even growing with no phosphate, and had the ability to adjust

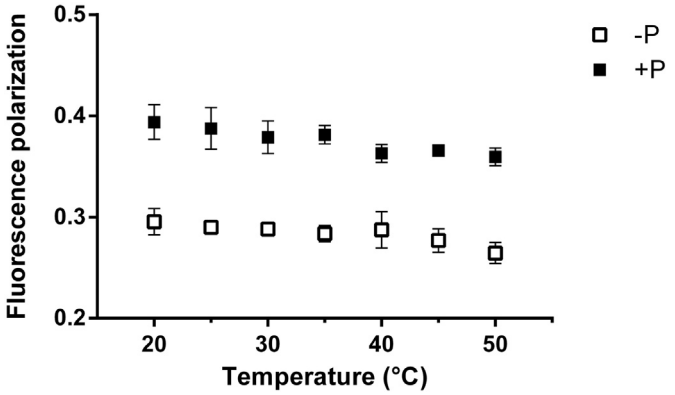

Fig. 6. Fluorescence polarization of DPH in thylakoid membranes isolated from *Synechococcus* sp. PCC 7942 cells. Cells under phosphate replete (+P) and phosphate depleted (−P) conditions were harvested on day 16. Mean, n = 3. The legends, +P and −P, indicate phosphate concentrations in the medium of 0.04 g L^{-1} and 0 g L^{-1}, respectively.

photosynthetic activities and light utilization (Fig. 1). The phosphate stress induced a stepwise adaptation mechanism, because a more complicated lipid remodeling process seemed to be operative under −P conditions [51]. By contrast, nitrate stress is a more severe stress, as nitrate limitation presumably relates to protein synthesis [51]. More recent reports have shown that phytoplankton can assimilate dissolved organic phosphorus by the enzymatic reaction of purple acid phosphatases (PAPs) and alkaline phosphatases (APs) to meet their phosphorus requirement [59,60]. Furthermore, cyanobacteria are able to enrich large amounts of inorganic PPBs in the form of granules (Fig. 5), with the physiological functions of stress response and cell division [54,55]. This strategy can help cells reduce their physiological phosphorus need by 50% in phosphate-starved conditions [61,62]. Above all, those mechanisms are essential for organisms to maintain growth in environments low in phosphate.

The phycobiliprotein fluorescence value contributes to the F_0 value in cyanobacteria, and may eliminate damage by dissipating excess light that cannot be used [34,44]. The parameter fluorescence emission ratio (phycoerythrin:phycocyanin), indicating the energy transfer rate between these two phycobiliproteins, has been adopted to evaluate cyanobacteria photosynthesis activity [34]. In our study the PE:PC ratio had a sharp turnover pattern under phosphate concentration of 0, 0.01, and 0.02 g L^{-1}, which was different from cells cultivated under other phosphate concentrations (Fig. 1D). This alteration suggests an adjustment of light utilization capacity under phosphate-starved conditions for *Synechococcus* sp. PCC 7942. Furthermore, the ratio of MGDG and DGDG is important for stability and normal function of the photosynthetic apparatus [10]. Our study found that the MGDG/DGDG ratio increased from day 8 (0.7) to day 16 (1.0) (calculated from Fig. 8A and B), which may also be related to the increased light utilization. The results demonstrate that cyanobacteria can survive in phosphate-starved conditions, which may also relate to membrane lipid changes.

4.2. Cyanobacteria only accumulate glycolipids under phosphate stress conditions

Typically, nitrogen [36] and phosphorus deficiency [63] as well as extreme environmental conditions, e.g. high salinity [64], high light intensity [65], or extreme temperatures [66] induce the accumulation of neutral lipids in most microalgae and higher plants. Neutral lipids (such as TAG) can serve as carbon and energy storage lipids when cell growth is arrested [51]. However, in our study, no significant accumulation of neutral lipids was observed in *Synechococcus* sp. PCC 7942 under phosphate-starved conditions (Fig. 3). Cyanobacteria have a strong ability to synthesize photosynthetic membranes, but they lack native DAG acyltransferases (DGAT) which catalyze TAG synthesis from DAG and acyl-CoA [67]. Although the proportion of neutral lipids in *Synechococcus* sp. PCC 7942 was > 50% of total lipids (Figs. 2 and 3), the main components might be pigments, DAG, FFA, and sterols [68,69]. Based on the TEM results, the increased thickness and superficial area of the thylakoid membrane in −P cells suggested an accumulation of glycolipids in cyanobacteria (Fig. 5). Consistent with our findings, photosynthetic bacterium *Rhodobacter sphaeroides* only accumulated glycolipids and betaine lipids under phosphate stress conditions [18]. It has also been reported that production of glycolipids and neutral lipids can both be induced under phosphate stress or other nutrient stress conditions in plants and some eukaryotic microalgae [63,70–72]. Hence, we suggest that cyanobacteria only accumulate glycolipids under phosphate stress conditions, which is different from plants and eukaryotic microalgae.

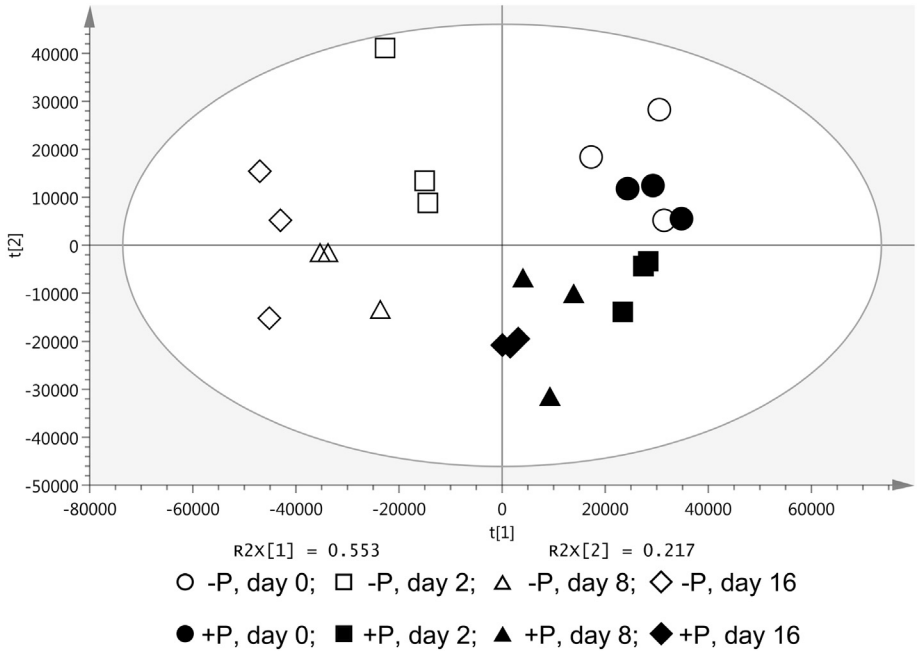

Fig. 7. The score scatter plot of PCA of membrane lipidome data in negative ions (ESI^-) mode. Cells under phosphate replete (+P) and phosphate depleted (−P) conditions were harvested on day 0, day 2, day 8, and day 16, successively. The legends, +P and −P, indicate phosphate concentrations in the medium of 0.04 g L^{-1} and 0 g L^{-1}, respectively.

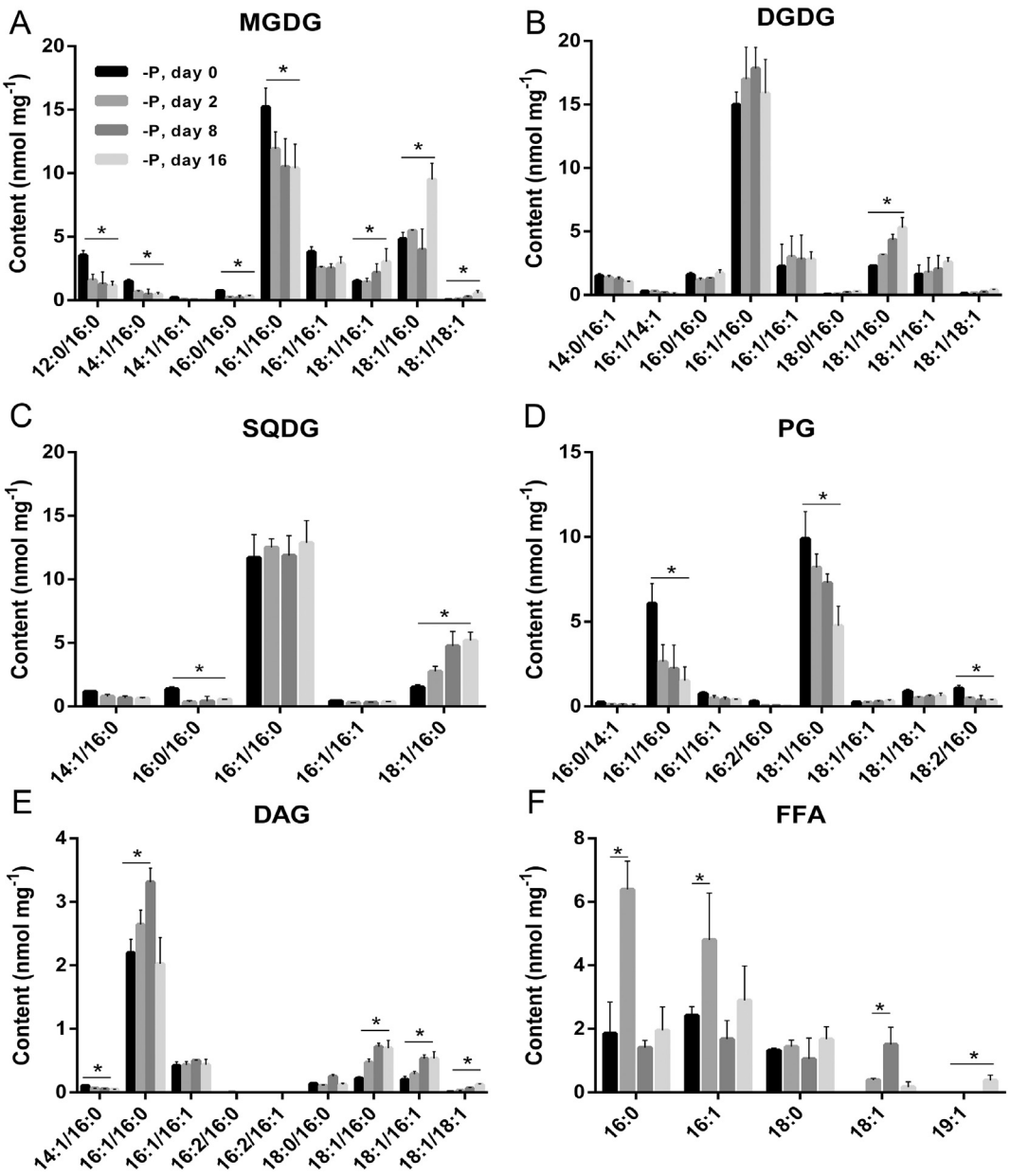

Fig. 8. The contents of molecular species of each lipid class in *Synechococcus* sp. PCC 7942 in phosphate depleted (−P) condition. Cells grown in modified BG11 medium in phosphate depleted (−P) condition for 0 day (control), 2 days, 8 days, and 16 days. Mean, n = 3. Student's *t*-test (*P < 0.05). The legend, −P, indicates phosphate concentration in the medium of 0 g L^{-1}.

Glycolipids and phospholipids are the main structural components of thylakoid and cytoplasmic membranes [45]. The increased glycolipid yields seem to be related to the replacement of phospholipids by non-phosphorus lipids, such as glycolipids (Figs. 2 and 3), which makes phosphorus available for other vital physiological metabolism processes. This effective phosphorus-conserving mechanism has been detected in many organisms during phosphate stress, including microalgae and photosynthetic bacteria [18,73]. In our study, the glycolipid content increased simultaneously with the reduction of chlorophyll content (Fig. 1B), indicating a protection machinery against photo oxidation and over excitation at high light intensity [26]. Above all, the present results imply that glycolipid accumulation under phosphate stress conditions may help cyanobacteria adapt to this unfavorable environment.

4.3. Phosphate-starvation adaptation by membrane lipid remodeling

Glycolipids (MGDG, DGDG, and SQDG) and phosphatidylglycerol (PG) are widely present in photosynthetic organisms and contribute to the construction of membrane systems [46–48]. The cyanobacterial thylakoid membranes are the predominant membrane, representing almost all cellular membranes [74]. In our study, DGDG and SQDG accumulated under phosphate-limited conditions (Fig. 4B), which was consistent with previous studies in plants [11,12,75] and microalgae [13,51,71]. Moreover, a diminished MGDG/DGDG ratio, from 2.2 (+P cells) to 1.2 (−P cells), was also detected (calculated from Fig. 4B). The MGDG/DGDG ratio (non-bilayer forming lipids/bilayer forming lipids) is important for the stability and normal functioning of the plastid membrane, and can be regulated by the availability of phosphorus [10,51,76,77]. A comparison of membrane lipid composition of six species of salt-tolerant (i.e., samphire [*Salicornia europaea*]) and -sensitive (i.e., cucumber [*Cucumis sativus*]) plants revealed that the MGDG/

DGDG ratio is correlated with the resistance to salt [78] and low temperature [79] in plants, which may function in protecting plants against stress. Thus, we infer that the ratio is also correlated with low-phosphate stress adaptation for cyanobacteria.

Furthermore, PG and SQDG are the only negatively charged membrane lipids and likely to have a similar function in the cell [80]. The DGDG accumulation during phosphate stress is similar to SQDG substitutes for PG in thylakoid membranes [12]. Hence, the degradation of PG by increasing amount of SQDG and DGDG (Fig. 4B) is an important mechanism for protecting thylakoid membranes. This membrane lipid remodeling where phospholipids are replaced by non-phospholipids is different in some organisms. Replacement of phospholipids by betaine lipids (BLs) has been shown in *C. reinhardtii* [81], *Nannochloropsis* [21], *Rhodobacter sphaeroides* [17,18] and *Sinorhizobium melilot* [19] under phosphate stress conditions. The results indicate that the accumulation of DGDG and SQDG are both necessary for phosphate adaptation of cyanobacteria.

4.4. Phosphate-starvation induce changes of membrane thickness and fluidity

Synechococcus sp. PCC 7942 seemed to contain only traces of medium-chain fatty acids (C12 and C14) and was C16 and C18 rich (Table 1). It is noteworthy that the fatty acids at the sn-2 position of membrane lipid molecular species are mainly C16 fatty acids in *Synechococcus* sp. PCC 7942 (Fig. 8), which has been proposed to maintain the structure and function of the photosynthetic protein and is preferred in freshwater cyanobacteria [82]. Compared with marine *Synechococcus* strains, i.e., *Synechococcus* sp. WH7803, which is C14 rich at the sn-2 position of membrane lipids [34], *Synechococcus* sp. PCC 7942 has a thicker thylakoid membrane. This feature is related to traits for adapting to phosphate stress, as a thicker membrane lipid may result in a stacked formation from hydrogen bond connections (Fig. 5B) [83]. This stacking not only balances the static electricity produced by charged lipids SQDG and PG, but also maintains a high hydrous stacked membrane [83].

A notable increase in content of C18 (especially C18:1) was observed in all glycolipids at the expense of C12 and C14 (Table 1), which also suggested a thicker membrane under −P conditions (Fig. 5B). Moreover, the saturated and monounsaturated C16 and C18 fatty acids contain higher caloric value than that of C12 and C14 [84], which may store more energy for cell survival [85]. We therefore speculate that the accumulation of glycolipids with high proportions of C16 and C18 fatty acids benefit energy saving, just as TAG accumulation does for eukaryotic microalgae [86]. Further, a large amount of C18:1 in membrane lipids triggered by phosphate stress was also found in several eukaryotic microalgae [87,88]. Increased C18:1 will lead to an elevation of unsaturated membrane lipids, which will directly affect membrane fluidity (Fig. 6), and further impact photosynthetic activities [34,56]. Above all, we suggest that increases of C18:1 in glycolipids may contribute to an appropriate membrane fluidity and function in phosphate adaptation.

4.5. Pathways of membrane lipid remodeling

Based on the UHPLC-MS(/MS) lipidomic data, a likely scenario for the fluxes of fatty acids and the DAG backbone is proposed in Fig. 9. Reduced PG 18:1:16:0, simultaneous with increased DGDG 18:1/16:0 and SQDG 18:1/16:0 with the same stereochemistry (Fig. 8B, C and D), strongly suggests a conversion of PG to DGDG and SQDG (Fig. 9). The total DAG content increased from 3.6 to 5.5 (nmol mg^{-1}) on day 8 and then gradually decreased to 4.1 (nmol mg^{-1}) on day 16 (calculated from Fig. 8E). This observation does not rule out the role of substrate (DAG) in the regulation of glycolipid synthesis, because the metabolism of DAG (by glycolipid assembly) and the supplement of DAG (by phospholipid degradation) are balanced during different growth stages under phosphate deprivation [89]. Phospholipase C (PLC) is involved in the lipid remodeling in bacteria *Sinorhizobium meliloti* [49]. A homologous gene has also been detected in yeast and *Agrobacterium* [89–91]. Thus, PLC may be involved in phospholipid degradation and DAG release under phosphate-starved conditions in our experiment. This observation has also been reported in phosphate-deprived plants and diatoms [13,75]. With the upregulation of PLC and phospholipase D (PLD), the increased DAG is suggested to act as substrate for synthesis of glycolipids (Fig. 9) [13,75]. Moreover, the content of DAG 16:1/16:0 was decreased by 39% from day 8 to day 16, which demonstrates the modification of DAG molecular species. This modification may be catalyzed by phosphatidylcholine:diacylglycerol cholinephosphotransferase (PDCT), generating new molecular species of DAG (Fig. 9) [92].

In addition, the initial significant degradation of MGDG 16:1/16:0 was consistent with the increase of DAG 16:1/16:0, suggesting a conversion from MGDG to DAG on day 2. Although this conversion route has been revealed in *Arabidopsis* freezing tolerance catalyzed by galactolipid:galactolipid galactosyltransferase/sensitive-to-freezing 2 (SFR2) [93], we could not observe the formation of other oligogalactolipids in *Synechococcus* sp. PCC 7942 and did not find the highest sequence similarity to SFR2 in *Synechococcus* sp. PCC 7942. Moreover, a sharp increase in content of total FFA by 125% was detected during the first two days of phosphate-starvation, which was also in line with the significant decrease of MGDG (Fig. 8). This demonstrated that MGDG may provide fatty acids under phosphate deprivation (Fig. 9). Similar with our results, in *Chlamydomonas*, FFAs are produced by an upregulation of the MGDG-specific lipase for TAG synthesis under nitrate deprivation [81,94]. Taken together, this data indicates that the initial degradation of MGDG in our experiment may provide fatty acids pools for DAG de novo synthesis (Fig. 9).

Hence, we propose that, in cyanobacteria, glycolipid accumulation and lipid remodeling come from two different pathways: (1) conversion of PG to glycolipids, and (2) degradation of MGDG for glycolipids de novo synthesis (Fig. 9).

5. Conclusions

The present study showed that *Synechococcus* sp. PCC 7942 can grow under phosphate depleted conditions, which is related to the DGDG and SQDG accumulation, and an increasing content of C18:1 fatty acid in glycolipids. This membrane lipid remodeling is likely to regulate membrane fluidity, and further impact the efficient photosynthetic activities. An overall study of the lipidome indicated that the accumulation of glycolipids and C18:1 fatty acids were primarily dependent on the contribution of PG and MGDG. The degradation of PG molecules (namely 16:1/16:0 and 18:1/16:0) were postulated to be converted to DAG with 16:0 at sn-2 position, and participated in DGDG and SQDG synthesis. Moreover, the initial reduction of MGDG molecules (namely 16:1/16:0, 14:1/16:0, 12:0/16:0, 16:0/16:0) were hydrolyzed into different acyl groups and provided an acyl pool to participate in DAG de novo synthesis and glycolipid assembly. This adaptation process in phosphate-starved *Synechococcus* sp. PCC 7942 addressed the pivotal roles of galactolipids and phospholipids in mediating fluxes of DAG backbones and fatty acids to the glycolipids.

Transparency document

The Transparency document associated with this article can be found, in online version.

CRediT authorship contribution statement

Zhou Peng: Investigation, Data curation, Visualization, Formal analysis, Writing - original draft.**Lei Feng:** Methodology, Validation.**Xiaoxue Wang:** Software.**Xiaoling Miao:**

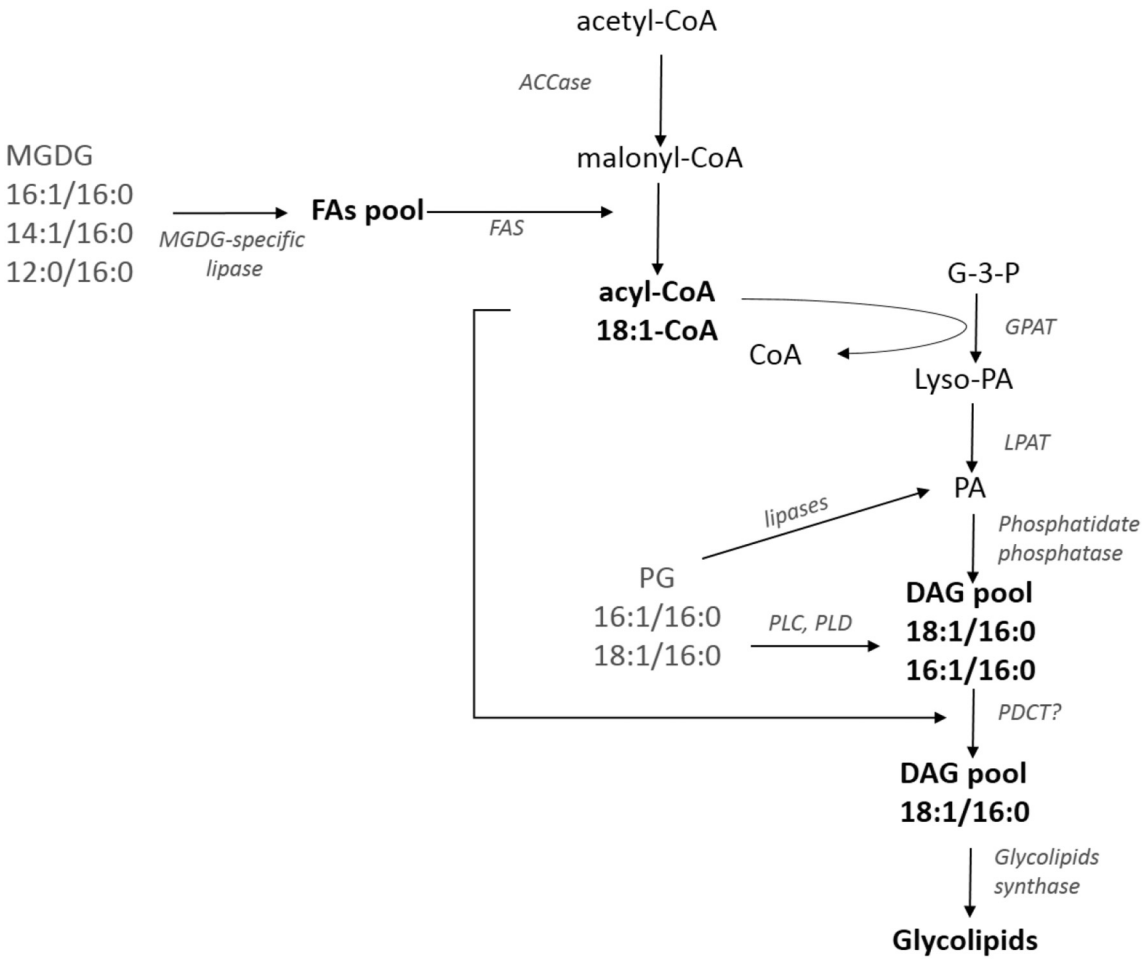

Fig. 9. A possible pathway for the membrane lipid remodeling mechanism in phosphate-deprived *Synechococcus* sp. PCC 7942. The route is based on the dynamic lipidomic alteration during 16 days of phosphate starvation in *Synechococcus* sp. PCC 7942. ACCase, acetyl-CoA carboxylase; FAS, fatty acid synthesis (FAS) complex; GPAT, glycerol-3-phosphate acyltransferase; LPAT, lysophosphatidyl acyltransferase; PDAT, phospholipid diacylglycerol acyltransferase; PDCT, PC:DAG cholinephosphotransferase; PLC, phospholipase C; PLD, phospholipase D; Glycolipids synthase in responsible for glycolipid synthesis from DAG, which includes five different enzymes (MgdA, monoglucosyldiacylglycerol synthase, MgdE monoglucosyldiacylglycerol epimerase; DgdA, digalactosyldiacylglycerol synthase, SqdB, UDP-sulfoquinovose synthase; SqdX, sulfoquinovosyldiacylglycerol synthase). Lipid molecules in dim grey color indicate a decreasing amount and in bold black indicate an increasing amount.

Conceptualization, Writing - review & editing, Supervision, Funding acquisition, Resources, Project administration.

Transparency document

The https://doi.org/10.1016/j.bbalip.2019.158522 associated with this article can be found, in online version.

Declaration of Competing Interest

The authors declare that they have no known competing financial interests or personal relationships that could have appeared to influence the work reported in this paper.

Acknowledgements

This research was financially supported by the National Natural Science Foundation of China (No. 41476122). It was also supported by the National High Technology Research and Development Program (863 Program) of China (No. 2013AA065805). We would also like to thank Dr. Ge Wang and Ruibin Wang (Instrumental Analysis Center of SJTU) for their excellent technical help.

Appendix A. Supplementary data

Supplementary data to this article can be found online at https://doi.org/10.1016/j.bbalip.2019.158522.

References

[1] G. Hölzl, P. Dörmann, Structure and function of glycoglycerolipids in plants and bacteria, Prog. Lipid Res. 46 (2007) 225–243, https://doi.org/10.1016/j.plipres.2007.05.001.
[2] M. Shimojima, H. Ohta, Critical regulation of galactolipid synthesis controls membrane differentiation and remodeling in distinct plant organs and following environmental, Prog. Lipid Res. 50 (2011) 258–266, https://doi.org/10.1016/j.plipres.2011.03.001.
[3] B.Z. Yu, W.Q. Li, Comparative profiling of membrane lipids during water stress in *Thellungiella salsuginea* and its relative *Arabidopsis thaliana*, Phytochem. 108 (2014) 77–86, https://doi.org/10.1016/j.phytochem.2014.09.012.
[4] B. Légeret, M. Schulz-Raffelt, H.M. Nguyen. P. Auroy, F. Beisson, G. Peltier, et al., Lipidomic and transcriptomic analyses of *Chlamydomonas reinhardtii* under heat stress unveil a direct route for the conversion of membrane lipids into storage lipids, Plant Cell Environ. 39 (2016) 834–847. doi:https://doi.org/10.1111/pce.12656.
[5] Y. Liang, K. Osada, Y. Sunaga, T. Yoshino, C. Bowler, T. Tanaka, Dynamic oi body generation in the marine oleaginous diatom *Fistulifera solaris* in response to nutrient limitation as revealed by morphological and lipidomic analysis, Algal Res. 12 (2015) 359–367, https://doi.org/10.1016/j.algal.2015.09.017.
[6] A. Kornberg, N.N. Rao, D. Ault-Riché, Inorganic polyphosphate: a molecule of many functions, Annu. Rev. Biochem. 68 (1999) 89–125, https://doi.org/10.1146/annurev.biochem.68.1.89.

[7] S.R. Mudge, A.L. Rae, E. Diatloff, F.W. Smith, Expression analysis suggests novel roles for members of the Pht1 family of phosphate transporters in *Arabidopsis*, Plant J. 31 (2002) 341–353, https://doi.org/10.1046/j.1365-313X.2002.01356.x.

[8] C.A. Ticconi, S. Abel, Short on phosphate: plant surveillance and countermeasures, Trends Plant Sci. 9 (2004) 548–555, https://doi.org/10.1016/j.tplants.2004.09.003.

[9] C.B. Taylor, P.A. Bariola, S.B. DelCardyre, R.T. Raines, P.J. Green, RNS2: a senescence-associated RNase of *Arabidopsis* that diverged from the S-RNases before speciation, Proc. Natl. Acad. Sci. 90 (1993) 5118–5122, https://doi.org/10.1073/pnas.90.11.5118.

[10] P. Dörmann, C. Benning, Galactolipids rule in seed plants, Trends Plant Sci. 7 (2002) 112–118, https://doi.org/10.1016/S1360-1385(01)02216-6.

[11] B. Essigmann, S. Güler, R.A. Narang, D. Linke, C. Benning, Phosphate availability affects the thylakoid lipid composition and the expression of SQD1, a gene required for sulfolipid biosynthesis in *Arabidopsis thaliana*, Proc. Natl. Acad. Sci. 95 (1998) 1950–1955, https://doi.org/10.1073/pnas.95.4.1950.

[12] H. Härtel, P. Dörmann, C. Benning, DGD1-independent biosynthesis of extraplastidic galactolipids after phosphate deprivation in *Arabidopsis*, Proc. Natl. Acad. Sci. 97 (2000) 10649–10654, https://doi.org/10.1073/pnas.180320497.

[13] A. Mühlroth, P. Winge, A.E. Assimi, J. Jouhet, E. Maréchal, M.F. Hohmann-Marriott, et al., Mechanisms of phosphorus acquisition and lipid class remodeling under P limitation in a marine microalga, Plant Physiol. 175 (2017) 1543–1559, https://doi.org/10.1104/pp.17.00621.

[14] Y. Okazaki, H. Otsuki, T. Narisawa, K. Makoto, S. Sawai, Y. Kamide, et al., A new class of plant lipid is essential for protection against phosphorus depletion, Nat. Commun. 4 (2013) 1510, https://doi.org/10.1038/ncomms2512.

[15] Y. Okazaki, K. Takano, K. Saito, Lipidomic analysis of soybean leaves revealed tissue-dependent difference in lipid remodeling under phosphorus-limited growth conditions, Plant Biotechnol. 34 (2017) 57–63, https://doi.org/10.5511/plantbiotechnology.17.0113a.

[16] K. Tawaraya, S. Honda, W. Cheng, M. Chuba, Y. Okazaki, K. Saito, et al., Ancient rice cultivar extensively replaces phospholipids with non-phosphorus glycolipid under phosphorus, Physiol. Plantarum 163 (2018) 297–305, https://doi.org/10.1111/ppl.12699.

[17] C. Benning, J.T. Beatty, R.C. Prince, C.R. Somerville, The sulfolipid sulfoquinovosyldiacylglycerol is not required for photosynthetic electron transport in *Rhodobacter sphaeroides* but enhances growth under phosphate limitation, Proc. Natl. Acad. Sci. 90 (1993) 1561–1565, https://doi.org/10.1073/pnas.90.4.1561.

[18] C. Benning, Z.H. Huang, D.A. Gage, Accumulation of a novel glycolipid and a betaine lipid in cells of *Rhodobacter sphaeroides* grown under phosphate limitation, Arch. Biochem. Biophys. 317 (1995) 103–111, https://doi.org/10.1006/abbi.1995.1141.

[19] I.M. López-Lara, J.L. Gao, M.J. Soto, A. Solares-Pérez, B. Weissenmayer, C. Sohlenkamp, et al., Phosphorus-free membrane lipids of *Sinorhizobium meliloti* are not required for the symbiosis with alfalfa but contribute to increased cell yields under phosphorus-limiting conditions of growth, Mol. Plant-Microbe Interact. 18 (2005) 973–982, https://doi.org/10.1094/MPMI-18-0973.

[20] C. Giroud, A. Gerber, W. Eichenberger, Lipids of *Chlamydomonas reinhardtii.* Analysis of molecular species and 711 intracellular site(s) of biosynthesis, Plant Cell Physiol. 29 (1988) 587–595, https://doi.org/10.1093/oxfordjournals.pcp.a077533.

[21] H. Murakami, T. Nobusawa, K. Hori, M. Shimojima, H. Ohta, Betaine lipid is crucial for adapting to low temperature and phosphate deficiency in *Nannochloropsis*, Plant Physiol. 177 (2018) 181–193, https://doi.org/10.1104/pp.17.01573.

[22] E.A. Devers, V. Wewer, I. Dombrink, P. Dörmann, G. Hölzl, A processive glycosyltransferase involved in glycolipid synthesis during phosphate deprivation in *Mesorhizobium loti*, J. Bacteriol. 193 (2011) 1377–1384, https://doi.org/10.1128/JB.00768-10.

[23] P. Flombaum, J. Gallegos, R. Gordillo, J. Rincon, L. Zabala, N. Jiao, et al., Present and future global distributions of the marine cyanobacteria *Prochlorococcus* and *Synechococcus*, Proc. Natl. Acad. Sci. 110 (2013) 9824–9829, https://doi.org/10.1073/pnas.1307701110.

[24] S. Levine, D. Schindler, Influence of nitrogen to phosphorus supply ratios and physicochemical conditions on cyanobacteria and phytoplankton species composition in the experimental lakes area, Canada. Can. J. Fish. Aquat. Sci. 56 (1999) 451–466, https://doi.org/10.1139/cjfas-56-3-451.

[25] B.A.S. Van Mooy, H.F. Fredricks, B.E. Pedler, S.T. Dyhrman, D.M. Karl, M. Koblížek, et al., Phytoplankton in the ocean use non-phosphorus lipids in response to phosphorus scarcity, Nature 458 (2009) 69–72, https://doi.org/10.1038/nature07659.

[26] B. Gašparović, J. Godrijan, S. Frka, I. Tomažić, A. Penezić, D. Marić, et al., Adaptation of marine plankton to environmental stress by glycolipid accumulation, Mar. Environ. Res. 92 (2013) 120–132, https://doi.org/10.1016/j.marenvres.2013.09.009.

[27] S. Güler, A. Seeliger, H. Härtel, G. Renger, C. Benning, A null mutant of *Synechococcus* sp. PCC 7942 deficient in the sulfolipid sulfoquinovosyl diacylglycerol, J. Biol. Chem. 271 (1996) 7501–7507, https://doi.org/10.1074/jbc.271.13.7501.

[28] B.A.S. Van Mooy, G. Rocap, H.F. Fredricks, C.T. Evans, A.H. Devol, Sulfolipids dramatically decrease phosphorus demand by picocyanobacteria in oligotrophic marine environments, Proc. Natl. Acad. Sci. 103 (2006) 8607–8612, https://doi.org/10.1073/pnas.0600540103.

[29] K. Endo, K. Kobayashi, H. Wada, Sulfoquinovosyldiacylglycerol has an essential role in *Thermosynechococcus elongatus* BP-1 under phosphate-deficient conditions, Plant Cell Physiol. 57 (2016) 2461–2471, https://doi.org/10.1093/pcp/pcw159.

[30] K. Awai, H. Watanabe, C. Benning, I. Nishida, Digalactosyldiacylglycerol is required for better photosynthetic growth of *Synechocystis* sp PCC 6803 under phosphate limitation, Plant Cell Physiol. 48 (2007) 1517–1523, https://doi.org/10.1093/pcp/pcm134.

[31] X. Wang, Z. Shen, X. Miao, Nitrogen and hydrophosphate affects glycolipids composition in microalgae, Sci. Rep. 6 (2016) 30145, https://doi.org/10.1038/srep30145.

[32] S.Y. Chiu, C.Y. Kao, M.T. Tsai, S.C. Ong, C.H. Chen, C.S. Lin, Lipid accumulation and CO_2 utilization of *Nannochloropsis oculata* in response to CO_2 aeration, Bioresour. Technol. 100 (2009) 833–838, https://doi.org/10.1016/j.biortech.2008.06.061.

[33] T. Marsac, N. Houmard, Complementary chromatic adaptation: physiological conditions and action spectra, Methods Enzymol. 167 (1988) 318–328, https://doi.org/10.1016/0076-6879(88)67037-6.

[34] J. Pittera, J. Jouhet, S. Breton, L. Garczarek, F. Partensky, E. Maréchal, et al., Thermoacclimation and genome adaptation of the membrane lipidome in marine *Synechococcus*, Environ. Microbiol. 20 (2017) 612–631, https://doi.org/10.1111/1462-2920.13985.

[35] M. Zhu, P.P. Zhou, L.J. Yu, Extraction of lipids from *Mortierella alpina* and enrichment of arachidonic acid from the fungal lipids, Bioresour. Technol. 84 (2002) 93–95, https://doi.org/10.1016/S0960-8524(02)00028-7.

[36] M.C. Damiani, C.A. Popovich, D. Constenla, P.I. Leonardi, Lipid analysis in *Haematococcus pluvialis* to assess its potential use as a biodiesel feedstock, Bioresour. Technol. 101 (2010) 3801–3807, https://doi.org/10.1016/j.biortech.2009.12.136.

[37] D.H. Tang, W. Hai, P.L. Li, X.L. Miao, J.J. Zhong, CO_2 biofixation and fatty acid composition of *Scenedesmus obliquus* and *Chlorella pyrenoidosa* in response to different CO_2 levels, Bioresour. Technol. 102 (2011) 3071–3076, https://doi.org/10.1016/j.biortech.2010.10.047.

[38] J. Su, M. Ye, Y. Lou, Z. Yang, T. Sun, R. Zhang, et al., Low-molecular-mass organic acid and lipid responses of *Isochrysis galbana* Parke to high temperature stress during the entire growth stage, Algal Res. 26 (2017) 93–103, https://doi.org/10.1016/j.algal.2017.06.011.

[39] A. Criscuolo, M. Zellerc, K. Cook, G. Angelidou, M. Fedorova, Rational selection of reverse phase columns for high throughput LC–MS Lipidomics, Chem. Phys. Lipids 221 (2019) 120–127, https://doi.org/10.1016/j.chemphyslip.2019.03.006.

[40] M. Yang, Y. Meng, Y. Chu, S. Xue, Qualitative and quantitative analyses of polar glycerolipids in *Chlamydomonas reinhardtii* based on LC-MS techniques, Chin. Bull. Bot. 53 (2018) 812–828. doi:10.11983/CBB17179.

[41] K. Kondo, Y. Ochiai, M. Katayama, M. Ikeuchi, The membrane-associated CpcG2-phycobilisome in *Synechocystis*: a new photosystem I antenna, Plant Physiol. 144 (2007) 1200–1210, https://doi.org/10.1104/pp.107.099267.

[42] J. Barber, R.C. Ford, R.A.C. Mitchell, P.A. Millner, Chloroplast thylakoid membrane fluidity and its sensitivity to temperature, Planta 161 (1984) 375–380, https://doi.org/10.1007/BF00398729.

[43] K.S. Mironov, R.A. Sidorov, M.S. Trofimova, V.S. Bedbenov, V.D. Tsydendambaev, S.I. Allakhverdiev, et al., Light-dependent cold-induced fatty acid unsaturation, changes in membrane fluidity, and alterations in gene expression in *Synechocystis*, Biochim. Biophys. Acta Bioenerg. 1817 (2012) 1352–1359, https://doi.org/10.1016/j.bbabio.2011.12.011.

[44] T. Ogawa, M. Misumi, K. Sonoike, Estimation of photosynthesis in cyanobacteria by pulse-amplitude modulation chlorophyll fluorescence: problems and solutions, Photosynth. Res. 133 (2017) 63–73, https://doi.org/10.1007/s11120-017-0367-x.

[45] T. Li, J. Xu, B.Y. Gao, W.Z. Xiang, A.F. Li, C.W. Zhang, Morphology, growth, biochemical composition and photosynthetic performance of *Chlorella vulgaris* (Trebouxiophyceae) under low and high nitrogen supplies, Algal Res. 16 (2016) 481–491, https://doi.org/10.1016/j.algal.2016.04.008.

[46] N. Sato, H. Wada, Lipid biosynthesis and its regulation in cyanobacteria, in: H. Wada, N. Murata (Eds.), Lipids in Photosynthesis, Essential and Regulatory Functions, Springer, Dordrecht, 2009, pp. 157–177.

[47] M. Shimojima, H. Ohta, Y. Nakamura, Biosynthesis and function of chloroplast lipids, in: H. Wada, N. Murata (Eds.), Lipids in Photosynthesis, Essential and Regulatory Functions, Springer, Dordrecht, 2009, pp. 35–55.

[48] R. Goss, C. Wilhelm, Lipids in algae, lichens and mosses, in: H. Wada, N. Murata (Eds.), Lipids in Photosynthesis, Essential and Regulatory Functions, Springer, Dordrecht, 2009, pp. 117–135.

[49] M. Zavaleta-Pastor, C. Sohlenkamp, J.L. Gao, Z. Guan, R. Zaheer, T.M. Finan, et al., *Sinorhizobium meliloti* phospholipase C required for lipid remodeling during phosphorus limitation, Proc. Natl. Acad. Sci. 107 (2010) 302–307, https://doi.org/10.1073/pnas.0912930107.

[50] Y. Nakamura, Phosphate starvation and membrane lipid remodeling in seed plants, Prog. Lipid Res. 52 (2013) 43–50, https://doi.org/10.1016/j.plipres.2012.07.002.

[51] H. Abida, L.J. Dolch, C. Mei, V. Villanova, M. Conte, A. Block, et al., Membrane glycerolipid remodeling triggered by nitrogen and phosphorus starvation in *Phaeodactylum tricornutum*, Plant Physiol. 167 (2015) 118–136, https://doi.org/10.1104/pp.114.252395.

[52] J.E. Tillberg, J.R. Rowley, Physiological and structural effects of phosphorus starvation on the unicellular green alga *Scenedesmus*, Physiol. Plantarum 75 (1989) 315–324, https://doi.org/10.1111/j.1399-3054.1989.tb04633.x.

[53] Z.K. Yang, J.W. Zheng, Y.F. Niu, W.D. Yang, J.S. Liu, H.Y. Li, Systems-level analysis of the metabolic responses of the diatom *Phaeodactylum tricornutum* to phosphorus stress, Environ. Microbiol. 16 (2014) 1793–1807, https://doi.org/10.1111/1462-2920.12411.

[54] J. Li, M. Dittrich, Dynamic polyphosphate metabolism in cyanobacteria responding to phosphorus availability, Environ. Microbiol. 21 (2019) 572–583, https://doi.org/10.1111/1462-2920.14488.

[55] Y. Seki, K. Nitta, Y. Kaneko, Observation of polyphosphate bodies and DNA during the cell division cycle of *Synechococcus elongatus* PCC 7942, Plant Biol. 16 (2014) 258–263, https://doi.org/10.1111/plb.12008.

[56] D.A. Los, K.S. Mironov, S.I. Allakhverdiev, Regulatory role of membrane fluidity in

gene expression and physiological functions, Photosynth. Res. 116 (2013) 489–509, https://doi.org/10.1007/s11120-013-9823-4.
[57] S. Kobayashi, M. Tsuzuki, N. Sato, Sulfite-stress induced functional and structural changes in the complexes of photosystems I and II in a cyanobacterium, *Synechococcus elongatus* PCC 7942, Plant Cell Physiol. 56 (2015) 1521–1532, https://doi.org/10.1093/pcp/pcv073.
[58] Q. He, H. Yang, L. Wu, C. Hu, Effect of light intensity on physiological changes, carbon allocation and neutral lipid accumulation in oleaginous microalgae, Bioresour. Technol. 191 (2015) 219–228, https://doi.org/10.1016/j.biortech.2015.05.021.
[59] S. Lin, R.W. Litaker, W.G. Sunda, Phosphorus physiological ecology and molecular mechanisms in marine phytoplankton, J. Phycol. 52 (2016) 10–36, https://doi.org/10.1111/jpy.12365.
[60] J.P. Cañavate, I. Armada, I. Hachero-Cruzado, Common and species-specific effects of phosphate on marine microalgae fatty acids shape their function in phytoplankton trophic ecology, Microb. Ecol. 74 (2017) 623–639, https://doi.org/10.1007/s00248-017-0983-1.
[61] S. Bertilsson, O. Berglund, D.M. Karl, S.W. Chisholm, Elemental composition of marine *Prochlorococcus* and *Synechococcus*: implications for the ecological stoichiometry of the sea, Limnol. Oceanogr. 48 (2003) 1721–1731, https://doi.org/10.4319/lo.2003.48.5.1721.
[62] J.M. Krauk, T.A. Villareal, J.A. Sohm, J.P. Montoya, D.G. Capone, Plasticity of N:P ratios in laboratory and field populations of *Trichodesmium* spp, Aquat. Microb. Ecol. 42 (2006) 243–253, https://doi.org/10.3354/ame042243.
[63] K. Liang, Q. Zhang, M. Gu, W. Cong, Effect of phosphorus on lipid accumulation in freshwater microalga *Chlorella* sp, J. Appl. Phycol. 25 (2013) 311–318, https://doi.org/10.1007/s10811-012-9865-6.
[64] I. Pancha, K. Chokshi, R. Maurya, K. Trivedi, S.K. Patidar, A. Ghosh, et al., Salinity induced oxidative stress enhanced biofuel production potential of microalgae *Scenedesmus* sp. CCNM 1077, Bioresour. Technol. 189 (2015) 341–348. doi:https://doi.org/10.1016/j.biortech.2015.04.017.
[65] H.D. Goold, S. Cuiné, B. Légeret, Y.X. Liang, S. Brugière, P. Auroy, et al., Saturating light induces sustained accumulation of oil in plastidal lipid droplets in *Chlamydomonas reinhardtii*, Plant Physiol. 171 (2016) 2406–2417, https://doi.org/10.1104/pp.16.00718.
[66] K. Chokshi, I. Pancha, K. Trivedi, B. George, R. Maurya, A. Ghosh, et al., Biofuel potential of the newly isolated microalgae *Acutodesmus dimorphus* under temperature induced oxidative stress conditions, Bioresour. Technol. 180 (2015) 162–171, https://doi.org/10.1016/j.biortech.2014.12.102.
[67] X. Wang, X. Xiong, N. Sa, S. Roje, S. Chen, Metabolic engineering of enhanced glycerol-3-phosphate synthesis to increase lipid production in *Synechocystis* sp. PCC 6803, Appl. Microbiol. Biotechnol. 100 (2016) 6091–6101. doi:https://doi.org/10.1007/s00253-016-7521-9.
[68] E.C. Rivera, V. Montalescot, M. Viau, D. Drouin, P. Bourseau, M. Frappart, et al., Mechanical cell disruption of *Parachlorella kessleri* microalgae: impact on lipid fraction composition, Bioresour. Technol. 256 (2018) 77–85, https://doi.org/10.1016/j.biortech.2018.01.148.
[69] S. Mishra, A. Tyagi, I.V. Singh, R.S. Sangwan, Changes in lipid profile during growth and senescence of *Catharanthus roseus* leaf, Braz. J. Plant Physiol. 18 (2006) 447–454, https://doi.org/10.1590/S1677-04202006000400002.
[70] J. Jia, D.X. Han, H.G. Gerken, Y.T. Li, M. Sommerfeld, Q. Hu, et al., Molecular mechanisms for photosynthetic carbon partitioning into storage neutral lipids in *Nannochloropsis oceanica* under nitrogen-depletion conditions, Algal Res. 7 (2015) 66–77, https://doi.org/10.1016/j.algal.2014.11.005.
[71] I. Khozin-Goldberg, Z. Cohen, The effect of phosphate starvation on the lipid and fatty acid composition of the fresh water eustigmatophyte *Monodus subterraneus*, Phytochem. 67 (2006) 696–701, https://doi.org/10.1016/j.phytochem.2006.01.010.
[72] R.E.H. Smith, M. Gosselin, G. Kattner, L. Legendre, S. Pesant, Biosynthesis of macromolecular and lipid classes by phytoplankton in the Northeast Water Polynya, Mar. Ecol. Prog. Ser. 147 (1997) 231–242, https://doi.org/10.3354/meps147231.
[73] P. Martin, B.A. Van Mooy, A. Heithoff, S.T. Dyhrman, Phosphorus supply drives rapid turnover of membrane phospholipids in the diatom *Thalassiosira pseudonana*, ISME J. 5 (2011) 1057–1060, https://doi.org/10.1038/ismej.2010.192.
[74] I. Sakurai, J.R. Shen, J. Leng, S. Ohashi, M. Kobayashi, H. Wada, Lipids in oxygen-evolving photosystem II complexes of cyanobacteria and higher plants, J. Biochem. (Tokyo) 140 (2006) 201–209, https://doi.org/10.1093/jb/mvj141.
[75] N. Gaude, Y. Nakamura, W.R. Scheible, H. Ohta, P. Dörmann, Phospholipase C5 (NPC5) is involved in galactolipid accumulation during phosphate limitation in leaves of Arabidopsis, Plant J. 56 (2008) 28–39, https://doi.org/10.1111/j.1365-313X.2008.03582.x.
[76] N. Gaude, C. Bréhélin, G. Tischendorf, F. Kessler, P. Dörmann, Nitrogen deficiency in Arabidopsis affects galactolipid composition and gene expression and results in accumulation of fatty acid phytyl esters, Plant J. 49 (2007) 729–739, https://doi.org/10.1111/j.1365-313x.2006.02992.x.
[77] W.P. Williams, The physical properties of thylakoid membrane lipids and their relation to photosynthesis, in: P.A. Siegenthaler, N. Murata (Eds.), Lipids in Photosynthesis: Structure, Function and Genetics, Kluwer Academic Publishers, Dordrecht, 1998, pp. 21–52.
[78] O. Hirayama, M. Mihara, Characterization of membrane lipids of higher plants different in salt-tolerance, Agric. Biol. Chem. 51 (1987) 3215–3221, https://doi.org/10.1080/00021369.1987.10868556.
[79] I. Nishida, N. Murata, Chilling sensitivity in plants and cyanobacteria: the crucial contribution of membrane lipids, Annu. Rev. Plant Physiol. Plant Mol. Biol. 47 (1996) 541–568, https://doi.org/10.1146/annurev.arplant.47.1.541.
[80] C. Benning, Biosynthesis and function of the sulfolipid sulfoquinovosyl diacylglycerol, Annu. Rev. Plant Physiol. Plant Mol. Biol. 49 (1998) 53–75, https://doi.org/10.1146/annurev.arplant.49.1.53.
[81] Z.Y. Du, B.F. Lucker, K. Zienkiewicz, T.E. Miller, A. Zienkiewicz, B.B. Sears, et al., Galactoglycerolipid lipase PGD1 is involved in thylakoid membrane remodeling in response to adverse environmental conditions in *Chlamydomonas*, Plant Cell 30 (2018) 447–465, https://doi.org/10.1105/tpc.17.00446.
[82] K. Okazaki, N. Sato, N. Tsuji, M. Tsuzuki, I. Nishida, The significance of C16 fatty acids in the sn-2 positions of glycerolipids in the photosynthetic growth of *Synechocystis* sp PCC 6803, Plant Physiol. 141 (2006) 546–556, https://doi.org/10.1104/pp.105.075796.
[83] B. Demé, C. Cataye, M.A. Block, E. Marechal, J. Jouhet, Contribution of galactoglycerolipids to the 3-dimensional architecture of thylakoids, FASEB J. 28 (2014) 3373–3383, https://doi.org/10.1096/fj.13-247395.
[84] A.M. Ruffing, H.D.T. Jones, Physiological effects of free fatty acid production in genetically engineered *Synechococcus elongatus* PCC 7942, Biotechnol. Bioeng. 109 (2012) 2190–2199, https://doi.org/10.1002/bit.24509/abstract.
[85] S.H. Park, J. Kyndt, K. Chougule, J.J. Park, J.K. Brown, Low-phosphate-selected *Auxenochlorella protothecoides* redirects phosphate to essential pathways while producing more biomass, PLoS One 13 (2018) e0198953, , https://doi.org/10.1371/journal.pone.0198953.
[86] M.A. Welte, A.P. Gould, Lipid droplet functions beyond energy storage, Biochim. Biophys. Acta Mol. Cell Biol. Lipids 1862 (2017) 1260–1272, https://doi.org/10.1016/j.bbalip.2017.07.006.
[87] S. Sonkar, N. Mallick, An alternative strategy for enhancing lipid accumulation in chlorophycean microalgae for biodiesel production, J. Appl. Phycol. 30 (2018) 2179–2192, https://doi.org/10.1007/s10811-018-1419-0.
[88] J.P. Cañavate, I. Armada, I. Hachero-Cruzado, Aspects of phosphorus physiology associated with phosphate-induced polar lipid remodelling in marine microalgae, Plant Physiol. 214 (2017) 28–38, https://doi.org/10.1016/j.jplph.2017.03.019.
[89] T. Geske, K.V. Dorp, P. Dörmann, G. Hölzl, Accumulation of glycolipids and other non-phosphorous lipids in *Agrobacterium tumefaciens* grown under phosphate deprivation, Glycobiol. 23 (2013) 69–80, https://doi.org/10.1093/glycob/cws124.
[90] Y. Wang, S. Zhang, Z. Zhu, H. Shen, X. Lin, X. Jin, et al., Systems analysis of phosphate-limitation-induced lipid accumulation by the oleaginous yeast *Rhodosporidium toruloides*, Biotechnol. Biofuels 11 (2018) 148, https://doi.org/10.1186/s13068-018-1134-8.
[91] K.K. Yadav, N. Singh, R. Rajasekharan, Response to phosphate deprivation in yeast cells, Curr. Genet. 62 (2016) 301–307, https://doi.org/10.1007/s00294-015-0544-4.
[92] P.D. Bates, J. Browse, The significance of different diacylgycerol synthesis pathways on plant oil composition and bioengineering, Front. Plant Sci. 3 (2012) 147, https://doi.org/10.3389/fpls.2012.00147.
[93] E.R. Moellering, B. Muthan, C. Benning, Freezing tolerance in plants requires lipid remodeling at the outer chloroplast membrane, Science 330 (2010) 226–228, https://doi.org/10.1126/science.1191803.
[94] X. Li, E.R. Moellering, B. Liu, C. Johnny, M. Fedewa, B.B. Sears, et al., A Galactoglycerolipid lipase is required for triacylglycerol accumulation and survival following nitrogen deprivation in *Chlamydomonas reinhardtii*, Plant Cell 24 (2012) 4670–4686, https://doi.org/10.1105/tpc.112.105106.